Silicon and metal nanotemplates: Size and species dependence of structural and electronic properties

G. K. Gueorguiev
Departmento de Física da Universidade, P-3004-516 Coimbra, Portugal

J. M. Pacheco
Centro de Física Teórica e Computacional and Departmento de Física da Faculdade de Ciências, Complexo Interdisciplinar da Universidade de Lisboa, Av. Prof. Gama Pinto 2, P-1649-003, Lisboa Codex, Portugal

(Received 18 June 2003; accepted 19 August 2003)

We utilize first-principles computer simulations to study the dependence on size (n) and species (M) of structural and electronic properties of clusters with stoichiometry $M\,\mathrm{Si}_n$. We investigate a total of 168 clusters comprising from 1 to 14 silicon atoms together with one transition metal atom among 12 different elements. It is found that all elements exhibit a very similar size-dependence for the cohesive energy, in which clusters with $n=7$, 12 appear as local maxima, with shapes which are found to be essentially independent of the transition metal atom. It is also found that the electronic properties of structurally equivalent clusters depend sensitively on the transition metal atom involved, providing the means to tailor specific properties when designing cluster assembled materials. © *2003 American Institute of Physics.* [DOI: 10.1063/1.1617977]

I. INTRODUCTION

Recently, there has been a significant amount of research concerning the synthesis of well-defined nanodevices in which small atomic clusters constitute the elementary building blocks.

Since silicon is currently the most important material for electronic devices which are under pressure for constant miniaturization, bare silicon clusters of small and intermediate size have received a lot of attention.[1–3] As such, their equilibrium structures are relatively well studied.

The production of nanosized cluster-assembled materials is usually based upon the creation of separated small clusters which are then combined into cluster molecules (eventually in bulk amounts). In this respect, materials based on silicon clusters, which may differ from normal silicon in several properties, could be applied to create new devices.[2,3]

Following this line, mixed silicon clusters containing atoms of other elements and especially of transition metals, when considered as elementary building blocks of new condensed phases, may exhibit new, albeit unusual, properties, different from those of the currently produced metal silicides which together with some silicon-transition metal solid solutions already have multiple applications particularly in the development of new devices for high-temperature electronics and as engineering materials for high-temperature coatings, integrated circuits, and special ceramics.

In what concerns mixed clusters of silicon and one transition metal, no significant advances have been made after the first experimental works[4,5] dedicated to the photophysical studies of bare and metal-containing silicon clusters. The reactions between a metal and silicon in a supersonic jet to form mixed silicon–metal clusters have been observed by using the technique of laser vaporization and supersonic expansion with metal carbonyl seeded carrier gas, plus laser photoionization time-of-flight mass spectrometry. These experimental studies indicate an enhanced stability of $M\,\mathrm{Si}_{15}$ and $M\,\mathrm{Si}_{16}$ clusters with $M=$ Cr, W, and Mo, remaining the stability of smaller $M\,\mathrm{Si}_n$ clusters still unclear.

More recently,[6] mixed silicon clusters were successfully synthesized in the laboratory, using a single transition metal atom as a nucleation site. These clusters, of stoichiometry $M\,\mathrm{Si}_n^+$, with $M=$ Ta, W, Re, Ir, exhibited abundance spectra in which clusters with 12 silicon atoms generally emerged as the most abundant, being typically associated with a ''sandwich''-like structure in which the 12 silicon atoms form two regular, parallel and aligned hexagons which enclose a single transition metal atom in their center of mass.[6–8] Theoretical studies showed similar geometries for CrSi_{12} (Ref. 9) and CuSi_{12} (Ref. 10). The persistence of high abundance for $M\,\mathrm{Si}_{12}^+$ together with the observed stability of dehydrogenated clusters lent support to the possibility of employing such clusters as building blocks for cluster-assembled materials (cf. however, Ref. 8) which, in view of the many industrial applications of the standard bulk forms $M\,\mathrm{Si}$, $M\,\mathrm{Si}_2$ and also $M_2\,\mathrm{Si}$, set high expectations on these new materials. To this end, knowledge of the structural and electronic properties of *neutral* $M\,\mathrm{Si}_n$ clusters as a function of the number n of silicon atoms and also as a function of the transition metal atom species M can provide instrumental help in the quest for this type of cluster assembled materials.

In this work we study structural and electronic properties of neutral $M\,\mathrm{Si}_n$ clusters by means of first-principles simulations within the framework of density functional theory (DFT) in its generalized gradient approximation. We study a total of 168 clusters corresponding to 12 different metal atoms and, for each element M in $M\,\mathrm{Si}_n$, values of n ranging from 1 up to 14 silicon atoms. The metal atoms chosen form a submatrix of the Periodic Table involving four sequences

(each with three elements) from the VI-B, VII-B, and VIII-B groups of the Periodic Table, namely, [Cr,Mo,W], [Mn, Tc,Re], [Fe,Ru,Os], and [Co,Rh,Ir]. It is found that these clusters exhibit regularities in their behavior as a function of n which may be used at profit in the design of cluster-based nanodevices. Indeed, it is found that, overall, clusters with $n=7$ and 12 emerge as more stable than their neighbors in size. Moreover, their geometries are—apart from minor distortions—independent of the transition metal species, a feature which applies as well to clusters with $n=5$. Of all transition elements studied, $n=10$ is the smallest size at which the transition metal atom becomes endohedral, a feature that is observed for $M=$ Fe and Co.

This paper is organized as follows: After a brief description of the theoretical methods and tools employed in this work, carried out in Sec. II, we present the main results, together with the corresponding discussion, in Sec. III. Section IV contains the main conclusions and future prospects.

II. THEORY

All simulations were carried out making use of the ADF package,[11] which performs density functional theory (DFT) calculations of atoms, molecules, and clusters, and implements the self-consistent solution of the Kohn–Sham equations via projection in a Slater-type orbital basis set. A frozen-core triple-zeta basis set augmented with two polarization functions was used for silicon, leaving four active valence electrons per atom. The transition metal atoms were described making use of a triple-zeta basis augmented with polarization functions, and we included as active not only the electrons of the valence shell but also semicore electrons. Except where explicitly stated, all calculations reported in this work were carried out in the generalized gradient approximation (GGA) available in ADF.[11]

Within such a framework we started to perform, for each transition metal element and for each value of n satisfying $1\leqslant n\leqslant 14$, a geometry optimization consisting of maximizing the absolute value of the cohesive energy of each cluster ($|E_{\mathrm{coh}}(n)|$) via a conjugate gradient technique, in order to determine the equilibrium geometry for each size. For each combination of n and M we determined which are the energetically most competitive structures. In a second stage of our optimization strategy, we look for the most stable of each local minimum detected for a given n. These ''cross-optimizations'' ensure a better sampling of the potential energy hypersurface associated with all the variety of clusters considered. At the end of such ''cross-optimizations'' and subsequent local minimization we selected for each cluster a few of the most stable shapes. In the third and final stage of the optimization process and within the same computational framework we applied random perturbations to the structures obtained in the previous stage, corresponding to random displacements of one or more atoms of the cluster with respect to their equilibrium positions. Obviously, such a treatment breaks any intrinsic symmetry of the structures. After each random perturbation, we reoptimized the structure without imposing any symmetry constraints. As a result some of the equilibrium structures are asymmetric, whereas for other M Si$_n$ the lowest energy conformations are highly symmetric. A smearing of the electron density over molecular orbitals in the neighborhood of the Fermi level was applied in the initial stages of the optimizations since for large heteronuclear clusters this approach speeds up and stabilizes the self consistent convergence inherent to LDA and GGA.

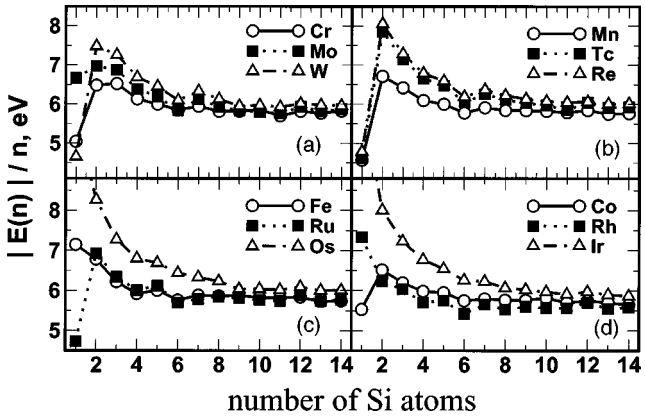

FIG. 1. Size and species dependence of cohesive energy. The absolute value of the cohesive energy ($|E_{\mathrm{coh}}(n)|$) divided by the number of silicon atoms (n) is plotted as a function of n. Each data point corresponds to the equilibrium geometry of a given cluster of stoichiometry M Si$_n$, for 12 different transition metal elements M and $1\leqslant n\leqslant 14$. The curves displayed in panels (a)–(d) comprise the elements indicated, belonging to groups VI-B, VII-B, and VIII-B of the Periodic Table. Each panel contains data from elements of the same group: The clusters for which the transition metal element has smallest atomic number Z are drawn with a solid line and open circles, those with intermediate value of Z with a dotted line and solid squares and the largest atomic number corresponds to the dotted–dashed line with open triangles.

Having obtained the set of atomic coordinates for the equilibrium structures, besides the cohesive energy, and within the referred *ab initio* framework, the ADF package allows one to carry out straightforward calculations of many other electronic properties such as the effective one-electron energies, HOMO-LUMO gap, bandwidth, etc.

III. RESULTS AND DISCUSSION

Since the absolute value of the cohesive energies does not allow a direct comparison of the relative stability of clusters with different number of Si atoms, in Fig. 1, panels (a)–(d) plot the results obtained for $|E_{\mathrm{coh}}(n)|$ divided by the number of silicon atoms (n). Maxima of the curves correspond to clusters displaying enhanced local stability. In each panel a specific group of three elements is displayed, such that clusters for which the transition element M has the smallest atomic number Z are drawn with a solid line and open circles, the intermediate value of Z with a dotted line and solid squares and the largest atomic number with the dotted–dashed line and open triangles. The layout of the data in Fig. 1 is organized by transition metal elements of the same group in the Periodic Table. It is noteworthy the remarkable similarities for the size-dependence of $|E_{\mathrm{coh}}(n)|/n$ both within each panel and across the four different panels. Overall, one observes that local maxima of $|E_{\mathrm{coh}}(n)|/n$ occur at the same sizes. Above $n=2$, $|E_{\mathrm{coh}}(n)|/n$ decreases monotonically as one increases n, up to $n=6$, after which $n=7$ emerges as a local maximum. A slower monotonic descent

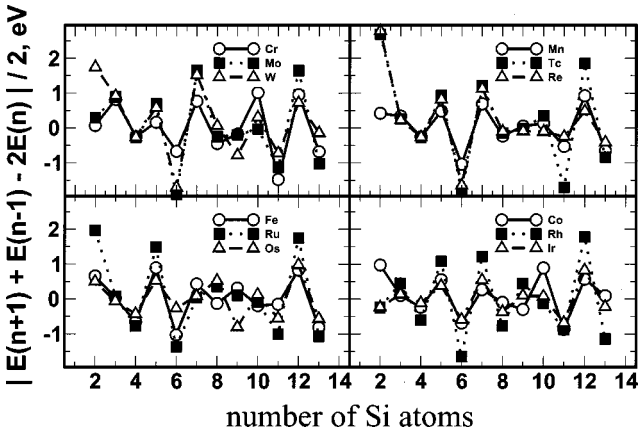

FIG. 2. The second difference spectra of cohesive energy $\Delta(n)$ plotted as a function of n for $2 \leqslant n \leqslant 13$ adopting the same notation of Fig. 1. By plotting $\Delta(n)$ one gets an enhancement of the local extrema hardly discernible in Fig. 1.

follows until a new minimum is reached at $n=11$, to be followed by another local maximum at $n=12$.

These features of the size-evolution are, as usual, best viewed by plotting the second difference spectra $\Delta(n)$ defined as

$$\Delta(n)=|E_{\mathrm{coh}}(n+1)+E_{\mathrm{coh}}(n-1)-2E_{\mathrm{coh}}(n)|/2, \qquad (1)$$

where $2 \leqslant n \leqslant 13$. In Fig. 2, panels (a)–(d), the size and species dependence of $\Delta(n)$ is shown. The notation of Fig. 2 is the same as Fig. 1. The extrema of the size-dependence of $\Delta(n)$, due to the differential character of this quantity, are sharpened. Consequently, the general trends of size and species dependence become sharper, in such a way that less well defined maxima, such as those at $n=5$ and $n=10$ for some transition metals, are now clearly observable. Overall, one observes that $n=7$ and $n=12$ are always associated with enhanced local stability, whereas for some elements also $n=5$ is locally stable.

These features common to all panels in Figs. 1 and 2 become even more remarkable if one plots the equilibrium shapes for selected values of n, as depicted in Fig. 3. Indeed, and apart from few exceptions (see below) the shapes of the clusters with $n=5$, 7, and 12 correspond to the shapes shown. As one changes the transition metal atom, one observes some minor distortions of the overall shape, which can be typically associated with small displacements of silicon atoms with respect to their location in the shapes depicted, scaled so as to reflect the presence of a different transition metal atom M. Indeed, by changing the transition metal atom, one is also changing the effective volume of the cluster, since the bond-length values tend to increase with the size of the transition metal atom.

Inspecting in greater detail the common shapes corresponding to $n=5$, 7, 12, in a total of 42 clusters, the most remarkable feature is associated with clusters with $n=7$, which not only exhibit local stability but also have the same geometry, the differences residing in the values of different bond lengths. For $n=12$ tiny distortions from the two perfectly aligned Si-hexagons were obtained for Tc, Ru, and Os, whereas Fe and Co show the largest distortions. These can,

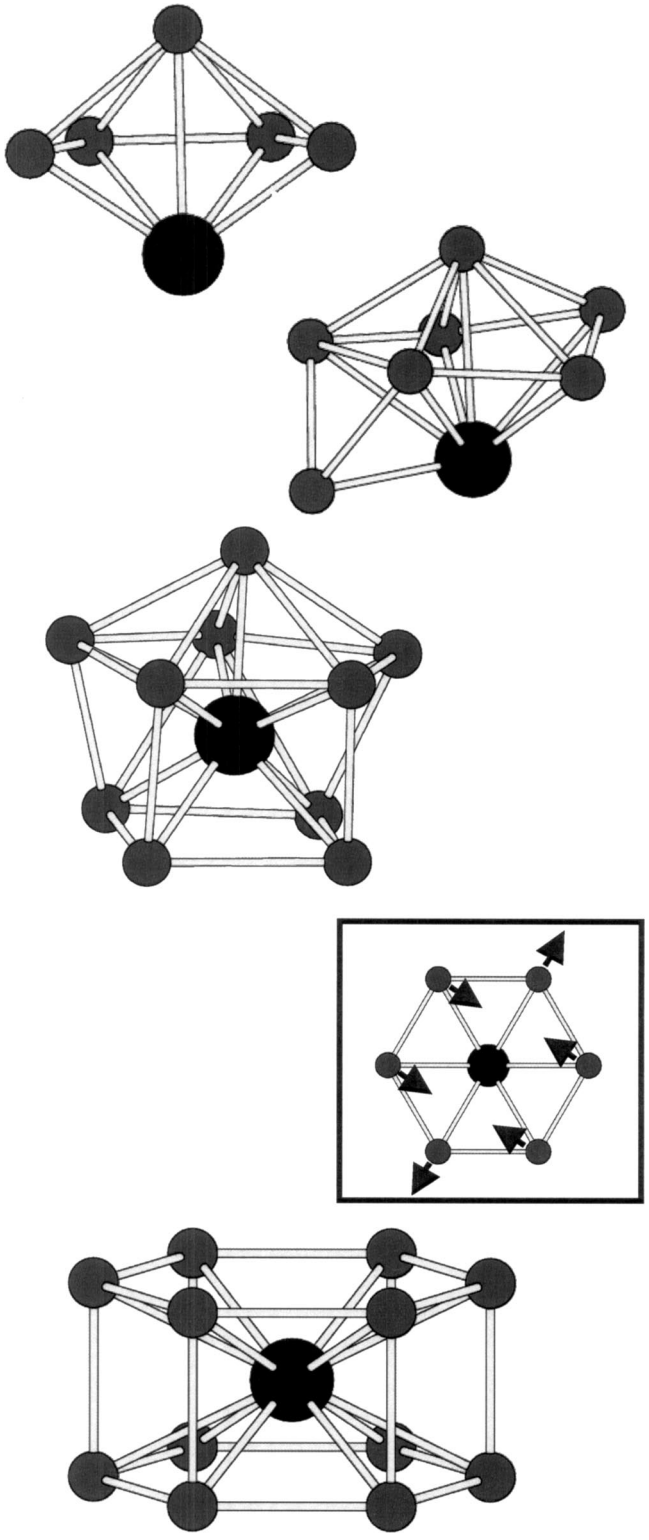

FIG. 3. Equilibrium shapes of M Si_n clusters. Clusters with $n=5$, 7, and 12 were found to display an equilibrium geometry which is almost independent of the transition metal element M. The typical shapes obtained as a result of the geometry optimization are illustrated here. From top to bottom are displayed: The capped trapezoid form typical of the clusters with $n=5$, the common conformation for $n=7$, the equilibrium shape of $CoSi_{10}$, the smallest value of n at which one finds an endohedral cagelike structure, and the emblematic hexagonal prism found for $n=12$. The inset illustrates the path which leads to the largest distortions from the ideal hexagonal prism with D_{6h} symmetry, obtained for $CoSi_{12}$ and $FeSi_{12}$ (see main text for details).

however, be summarized qualitatively with the help of the inset in Fig. 3: starting from the symmetric shape, we can view the resulting distortion by imagining the Si-atoms of one hexagon to move along the directions indicated by the arrows shown in the inset, whereas the Si-atoms of the second hexagon move the opposite way. The magnitude of these distortions is, on average, of 6.2% for Co and 5.5% for Fe,[12] being larger than any distortions perpendicular to the hexagonal planes. For $n=5$ we also have that 10 out of the 12 elements studied exhibit the structure depicted in Fig. 3, in which a trapezoid of four Si-atoms lies above the transition metal atom, being capped with the fifth Si-atom. From transition metal element to transition metal element one obtains differences in the distance from the metal atom to the trapezoidal plane, as well as in the bond-lengths within the trapezoid. For Co and Rh we obtain more symmetric structures, in which the trapezoid becomes a nice square for Co, being slightly distorted for Rh. Clusters with $n=3$ are also found to exhibit some regularities in what concerns their equilibrium shapes, since 8 out of the 12 structures exhibit a triangular pyramid shape, whereas the remaining four are planar, and were obtained for Rh, Ru, Co, and Fe.

Finally, we would like to point out that, for $n<12$, all equilibrium structures obtained place the transition metal element at an edge of the cluster, except for $CoSi_{10}$ and $FeSi_{10}$, for which we obtain the structure shown in Fig. 3. Whereas energetically these structures are not particularly favored, it is nevertheless quite remarkable that one may obtain an endohedral structure with only 10 silicon atoms.

Summarizing we can state that, for $n=5$, 7, and 12, we obtain a typical shape irrespective of the transition metal element. This is a very exciting result, taking into account the prospects of utilizing clusters of this type as templates in the synthesis of cluster assembled materials.

A central goal in the design of cluster assembled materials (besides the structural properties one may extrapolate from the constituent template) are the electronic properties one wants to obtain as one packs the simple cluster template to generate a more extended nanodevice. Will the remarkable structural regularities obtained persist when studying the electronic properties?

We addressed this issue by studying one electronic property which, at the level of single clusters provides important guidance in what concerns any extended phase—the HOMO-LUMO gaps, that is, the energy difference between the highest occupied molecular orbital and the lowest unoccupied molecular orbital. Since our extended calculations on $M\ Si_n$ clusters have been carried out within spin-unpolarized GGA (see below), only the clusters represented in panels (a) and (c) of Fig. 1 have finite HOMO-LUMO gaps. Figure 4 shows the evolution of the HOMO-LUMO gaps as a function of n, using the same notation as in Fig. 1. Direct inspection of Fig. 4 shows that, for the values of n at which one has found common structures for all 12 transition metal elements, one obtains different values for the HOMO-LUMO gaps. In accord with the underlying organization of the Periodic Table, one obtains that clusters of elements of the same group display similar HOMO-LUMO gaps, except for Fe, which seems to be ''out of phase'' with Ru and Os. The transition

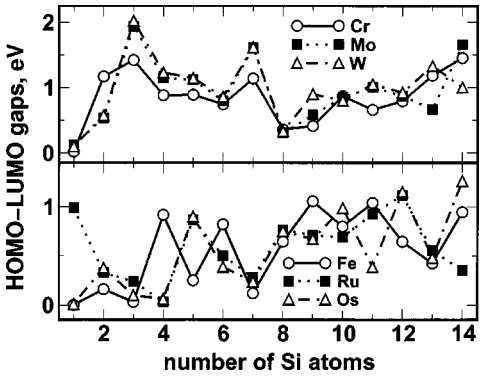

FIG. 4. Size and species dependence of HOMO-LUMO gaps. The size-evolution of the HOMO-LUMO gaps of $M\ Si_n$ clusters as a function of M and n is shown adopting the same notation of Fig. 1. The upper panel displays the data for those elements of panel (a) in Fig. 1, whereas the lower panel shows the curves corresponding to the elements of panel (c) in Fig. 1.

metal elements of group VI-B have larger HOMO-LUMO gaps than those of group VIII-B, in such a way that a sizable range of values for the HOMO-LUMO gaps is possible—compare, e.g., the HOMO-LUMO gaps for $n=5$, 7, 12—that is, for clusters exhibiting the same structural order. Obviously, to the extent that one can produce stable extended phases based on cluster units such as the ones studied here, one has quite a range of possibilities in synthesizing materials with different predefined properties.

Spin effects: Generally speaking, spin is well known to play important role in the physics and chemistry of transition metals. The question is whether this remark applies to clusters containing only *one* transition metal atom. In order to provide an answer to this question we carried out spin-polarized DFT calculations for some of the elements considered here. It should be noticed that such calculations are much longer and harder to converge than the spin-unpolarized ones already addressed. Four elements: Mo, Fe, Co, and Rh were chosen for these test calculations—$CoSi_n$ and $RhSi_n$ are gapless in the sense of Fig. 4, whereas $FeSi_n$ and $MoSi_n$ are good examples of cases for which one expects spin to play a role. We ran the calculations for values of n from 2 to 13, and the results confirm that the spin-polarized results follow very closely their spin-unpolarized counterparts, providing no new insights in the above results. Indeed, in what concerns the size-dependence of the cohesive energy, as one can see from Fig. 5, the spin-polarized curves basically follow the behavior shown in Fig. 1, with *no* implications for the discussions carried out above. Considering the HOMO-LUMO gaps, obviously one must distinguish between the (spin-unpolarized) closed-shell clusters containing Mo and Fe and the open-shell clusters $CoSi_n$ and $RhSi_n$. For $MoSi_n$ and $FeSi_n$, again the systematics shown in Fig. 4 is very nicely reproduced by the spin-polarized calculations, with the largest difference occurring, for both elements, for $n=10$.[12] In what concerns the open-shell clusters associated with Co and Rh, the difference here is obvious, since now a (more physical) finite HOMO-LUMO gap is obtained. In particular, we obtain a large HOMO-LUMO gap of nearly 1.5 eV for $CoSi_{10}$.

Overall, these test calculations indicate that spin effects

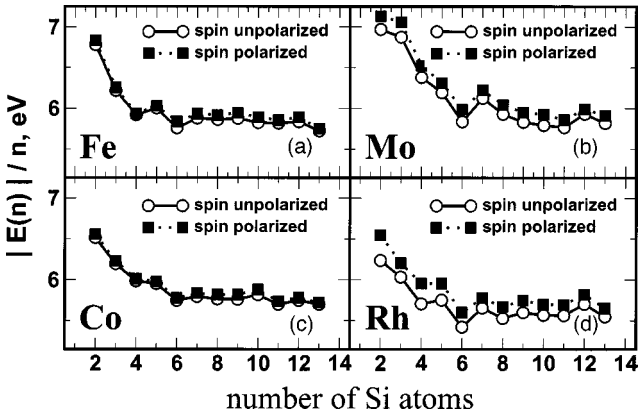

FIG. 5. Size and species dependence of cohesive energy—a comparison between spin-unpolarized and spin-polarized results obtained in test calculations performed for $FeSi_n$, $MoSi_n$, $CoSi_n$, and $RhSi_n$ [panels (a)–(d), respectively]. The spin-unpolarized results are drawn with open circles and solid lines whereas the spin-polarized data corresponds to solid squares connected with dashed lines.

do not play a relevant role in the characterization of the properties addressed here. This is certainly due to the fact that each cluster has only one transition metal atom.

IV. CONCLUSIONS

In summary, we investigated the size and species dependence of clusters of type $M\,Si_n$ where M stands for one out of 12 transition metal elements and $1 \leqslant n \leqslant 14$. Our work made use of first-principles computer simulations within the GGA to DFT. We found that the size-dependence of the cohesive energy of these clusters exhibited extrema at the same sizes, independently of the transition metal element involved—in particular, $n=7$, 12 are associated with locally stable clusters as a function of n. Furthermore, the equilibrium shapes associated with these locally stable structures are also independent of the transition metal. Nonetheless, it is found that irrespective of the regularities found for these structural properties, a prototypical electronic property, such as the HOMO-LUMO gap, exhibits a size and species dependence which can be qualitatively organized in a way similar to the organization of the transition metal elements in the Periodic Table. From this study one can establish a rather simple yet rich picture of the $M\,Si_n$ clusters as exhibiting a tendency to self-organize structurally in a way which is essentially independent of the transition metal. Since the shapes associated with clusters with the same selected value of n but with different M are remarkably similar, one obtains that structurally equivalent clusters exhibit electronic properties which depend on the transition metal element M. It remains a challenge to investigate the feasibility of assembling clusters together in more complex and extended nanodevices. Work along these lines is in progress.

ACKNOWLEDGMENTS

Financial support from the Portuguese Ministry of Science and Technology under Contract No. POCTI/C/FIS/10019/98 is gratefully acknowledged. G.K.G. acknowledges support from the Portuguese Foundation for Science and Technology under the Ph.D. Fellowship PRAXIS XXI/BD/19578/99.

[1] During the recent years an impressive amount of research has been devoted to this field. For a recent account see Refs. 2 and 3, and references therein.
[2] K.-M. Ho, A. A. Shvartsburg, B. Pan, Z.-Y. Lu, C.-Z. Wang, J. G. Wacker, J. Fye, and M. F. Jarrold, Nature **392**, 582 (1998).
[3] E. C. Honea, A. Ogura, D. R. Peale, C. Félix, C. A. Murray, K. Raghavachari, W. O. Sprenger, M. F. Jarrold, and W. L. Brown, J. Chem. Phys. **110**, 12161 (1999).
[4] S. M. Beck, J. Chem. Phys. **90**, 6306 (1989); **87**, 4233 (1987).
[5] S. M. Beck, Adv. Met. Semicond. Clusters **1**, 241 (1993).
[6] H. Hiura, T. Miyazaki, and T. Kanayama, Phys. Rev. Lett. **86**, 1733 (2001).
[7] T. Miyazaki, H. Hiura, and T. Kanayama, Phys. Rev. B **66**, 121403 (2002).
[8] J. M. Pacheco, G. K. Gueorguiev, and J. L. Martins, Phys. Rev. B **66**, 033401 (2002).
[9] S. N. Khanna, B. K Rao, and P. Jena, Phys. Rev. Lett. **89**, 016803 (2002).
[10] C. Xiao, F. Hagelberg, and W. A. Lester, Jr., Phys. Rev. B **66**, 075425 (2002).
[11] G. te Velde, E. J. Baerends, J. Comput. Phys. **99**, 84 (1992).
[12] Additional information, including numerical data and all the geometries for all clusters is available online at http://aloof.cii.fc.ul.pt/MSin/